RESEARCH PAPER

Effect of Process Parameters on Thermo-Mechanical Behavior of Extrusion of Aluminum Alloy

Yogesh Dewang[1*] and Vipin Sharma[2]

** dewang.yogesh3@gmail.com*

Received: January 2020 Revised: November 2020 Accepted: December 2020

[1] Associate Professor, Department of Mechanical Engineering, Lakshmi Narain College of Technology, Bhopal, India

[2] Associate Professor, Department of Mechanical Engineering, Sagar Institute of Research Technology & Science, Bhopal, India

DOI: 10.22068/ijmse.18.1.3

Abstract: *Finite element analysis has been carried out to investigate the effect of various parameters on axisymmetric hot extrusion process using aluminum alloy. The objective of the present work is to investigate the effect of friction coefficient, die angle, die-profile radius and predefined temperature of workpiece through FEM simulation of extrusion process. Nodal temperature distribution, heat flux, peak temperature at nodes and peak flux induced are identified as the output variables to assess the thermo-mechanical deformation behavior of aluminum alloy. Mesh sensitivity analysis is performed for the evaluation of mesh convergence as well as depicts the accuracy of present FEM model. The higher the coefficient of friction between interacting surfaces of die-billet assembly, the higher will be the increment in nodal temperature in billet. The higher the coefficient of friction, the higher will be the generation of heat flux within billet, as this is achieved for highest coefficient of friction. Peak nodal temperature diminishes with increase in die profile radius nearly by 17 %.Maximum heat flux diminishes non-linearly by 30% with increase in die profile radius. Maximum nodal temperature increases nearly linearly by 14% with increment in predefined temperature of billet. Maximum heat flux decreases non-linearly by 5 % with increment in the initial temperature of workpiece. Validation of present numerical model is established on the basis of deformation behavior in terms of evolution of nodal temperature distribution upon comparison with previous studies available in literature.*

Keywords: *Extrusion, Friction coefficient, Die-angle, Temperature, Flux, Finite Element Method (FEM).*

1. INTRODUCTION

Aluminum alloy extruded profiles are extensively used in automotive and aerospace applications owing to high strength to weight ratio, corrosion resistance, ease of fabrication, and low cost [1-3]. The extruded profiles are fabricated by an important metal forming process known as extrusion. In the extrusion, block of metal or billet is forced to flow by compressive forces through a die opening [4]. There are varieties of extrusion process such as direct, indirect, cold, hot etc. are used for profile fabrication. The hot extrusion is mainly used to produce aluminum alloy profiles of specific cross-sectional shapes. In the hot extrusion, preheated aluminum alloy billet are extruded through die orifices to form profiles [5-7]. In extruded profiles, the deformed grain structure resulted in superior mechanical properties, high fatigue strength and stress corrosion cracking resistance [8-9].

Investigations had carried out in the past decades for the analysis of extrusion process by adopting various methodologies. Mulji and Mackley [10] recognized the dependence of extrusion pressure developed within dies on area reduction and land length. In another FEM analysis of hot extrusion process of aluminum alloy composite, Akhgar et al [11] found that temperature evolution is highly influenced by extrusion speed and initial temperature. Rattanochaikul et al.[12] determined that plunger speed and solid fraction of the slurry have a profound effect on deformation behavior of aluminum 356 alloy. During FEM simulation of backward extrusion process Arbinia and Orangi [13] found considerable differences in velocity vectors lead to the distortions in hollow sections with thin walls and large reductions. Parvizian et al. [14] gathered decrement in subgrain size in die exit area and areas near to die in absence of friction and found dead material zone through FEM simulation of extrusion of aluminium alloy due to application of friction. Chen et al. [15] found increment of flow stress due to increment of dislocation while decrement in flow stress at

[Downloaded from herasat.iust.ac.ir on 2025-07-19]

[DOI: 10.22068/ijmse.18.1.3]

elevated temperatures during extrusion of aluminium alloy 7075 both through experiments and FEM simulation. Kapadia and Desai [16] reviewed the die extrusion process and suggested that extrusion of stainless steel tube was computationally challenging in simulation studies. They asserted that stainless steel tube extrusion is subjected to high strain rates, large deformations and high temperatures due to which there computational simulation study is a challenging task. Dong et al. [17] determined the temperature range for best performance of AA6N01 as 773-823 K during extrusion process after application of dynamic material model. Ramezani and Neitzert [18] conducted FEM simulation of Ti-6Al-4V alloy conical die extrusion process at elevated temperatures and investigated the effect of process parameter on stress-strain distribution, maximum ram speed and maximum applied pressure. They found that maximum ram force and maximum contact pressure decreases at higher die angles. Hodja et al. [19] attempted the FEM simulation of hybrid forward extrusion process through coupled and uncoupled procedure and found that resistively heated samples exhibit various temperatures at local positions after completion of process Wang et al. [20] realized that deformation resistance decreases with increment in deformation temperature of AZ31 magnesium alloy during hot extrusion process. In order to obtain uniform products during multi-hole extrusion process, Sahu et al. [21] recommended that die length and extrusion length are highly influential parameters. Zhou et al. [22] proposed a new approach named after differential velocity sideways extrusion (DVSE) approach which is capable of forming extrusion billets into curved profiles through extrusion and bending in joint manner with no sign of defects. Zhang et al. [23] noticed flow of material has a considerable influence on temperature field in friction extrusion process through numerical simulation. Yu et al. [24] observed that secondary phase of microstructure transformed to appreciably homogenous with increment in rotary revolutions during rotary extrusion process. Chen et al. [25] gathered that content of fine Mg17Al12 has decreased with increment of velocity of ram during hot extrusion process of AZ91 alloy. Kuboki et al. [26] obtained a spiral angle of 240 for hot tube extrusion of aluminium alloy 1100 and recommended improved efforts are required for enhancement of spiral angle. Kathirgamanathan and Neitzert [27] explored the effect of temperature, stress, strains and velocity changes during the extrusion of aluminum alloy through FEM simulation. Yadav et al. [28] explored the influence of friction coefficient, die angle and die profile radius on maximum nodal temperature, maximum contact pressure, and deformation during extrusion of aluminum alloy through FEM simulation. Liu et al. [29] realized an increment in torque with decrement in hole diameter for formation of internal threads in extrusion of AZ91D magnesium alloy. Preedawiphat et al. [30] recognized grain boundary as one of the vital factor for single-grain conditions which significantly influence the mechanism of curvature during micro-extrusion process. Ataei et al. [31] found that concurrent increment in friction coefficient and die angle have a profound influence over plastic deformation during severe plastic deformation by rectangular extrusion ,which results in increment in total accumulated strain. Park et al. [32] found the arbitrary Lagrangian- Eulerian formulation efficient enough to capture the effect of large deformation, strain rate and temperature during FEM analysis of extrusion process. Namburi et al. [33] found through FEM simulation of Aluminum 1100 alloy that die angle is a major parameter which helps in reduction of extrusion force. Shukur and Jaber [34] noticed through experimental and FEM analysis that forming load rises with increment in ram speed and die angle in extrusion process. Nouri et al. [35] found greater strain in second state rather than in first state during FEM simulation of twist extrusion process owing to evolution of peak shear strain and frictional effects. Davoudinejad et al. [36] claimed that FEM model is efficient enough for accurate prediction of cracks and distribution of stress in additively manufactured die during extrusion process. The objective of the present work is to investigate the effect of friction coefficient, die angle, die profile radius and predefined temperature of workpiece through FEM simulation of extrusion process using aluminum alloy. The results of the FEM simulation are presented in nodal temperature distribution, heat flux, peak temperature at nodes and peak flux induced.

[Downloaded from herasat.iust.ac.ir on 2025-07-19]

[DOI: 10.22068/ijmse.18.1.3]

2. EXPERIMENTAL PROCEDURES

Thermo-mechanical behavior of aluminium alloy for extrusion process has been derived through compression testing under various input temperatures. The experimental testing has been carried out at a strain rate of 0.1 s^{-1}. True stress versus true strain curves for aluminium alloy has been shown in Fig. 1. Thermo-mechanical properties are required for FEM analysis and are given in Table 1.The geometry of axisymmetric direct extrusion process mainly consist of two parts i.e. die and workpiece as shown in Fig. 2. In the present work, die is modelled herein as isothermal rigid body in which there are no changes in temperature as well as in geometry of die. Table 2 gives details of essential dimensions of extrusion die and workpiece. Fig. 3 shows Finite element model (FEM) model of axisymmetric direct extrusion process which consists of deformable workpiece of AA 6063 and isothermal rigid die. Both isothermal rigid die and billet are meshed with 36 and 1530 CAX4T elements respectively.

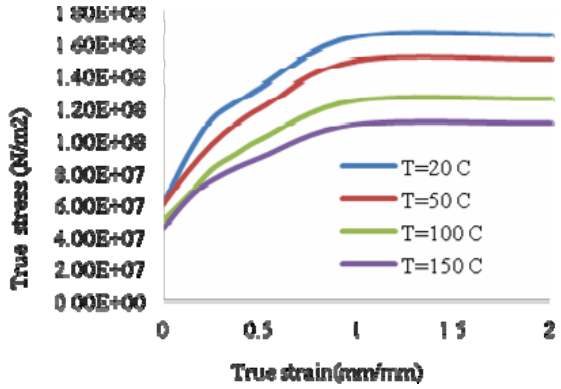

Fig. 1. Stress-strain relationships under various operating conditions for aluminium alloy [28].

Table 1. Thermo-mechanical properties of aluminium alloy [28].

Serial No.	Property of material	Magnitude
1	Density of material	2700 kg/m^3
2	Modulus of Elasticity	69 GPa
3	Poisson's coefficient	0.33
4	Thermal Conductivity	225 W/m-K
5	Specific heat	880 J/kg/k
6	Coefficient of thermal expansion	8.42×10^{-5} K^{-1}

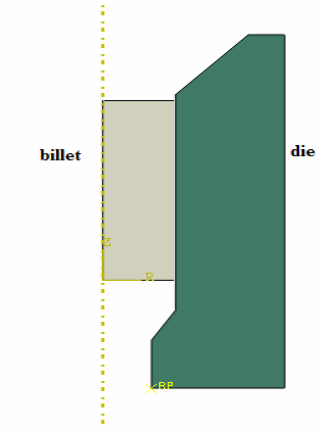

Fig. 2. Geometric model

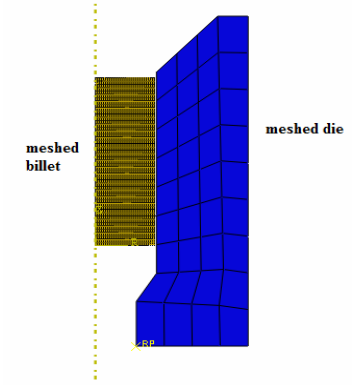

Fig. 3. FEM model

Table 2. Input process parameters for extrusion process [28].

Serial No.	Input process parameters	Magnitude
1	Angle of die (α)	56.5 degree
2	Opening radius(R_i)	70 mm
3	Radius of billet(R_o)	100 mm
4	Length of billet (L_o)	300 mm

In the present work, five different mesh sizes of workpiece are considered for mesh convergence study. Fig. 4 shows the different mesh sizes for mesh convergence study for workpiece. The five different mesh sizes are designated as 30×10, 40×20, 50×30, 60×40 and 70×50.The first value of mesh size represents the number of elements along vertical dimension i.e., length of initial billet (L_0) while second value of mesh size represents the number of elements along initial radius of workpiece before deformation (R_o).In each case of mesh size, ten elements are increased in both dimensions of workpiece.

[Downloaded from herasat.iust.ac.ir on 2025-07-19]

[DOI: 10.22068/ijmse.18.1.3]

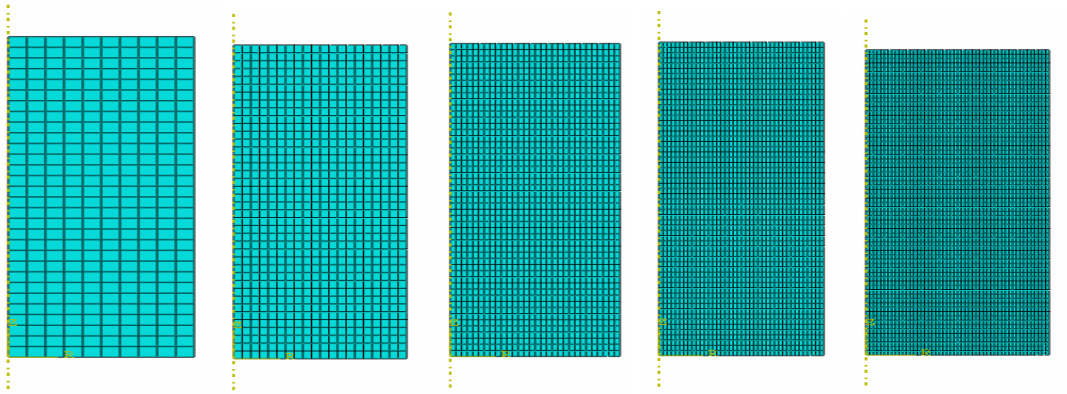

Fig. 4. (a-e) Different mesh sizes used in the axisymmetric direct extrusion process for mesh convergence study.

The results of mesh convergence are presented in form of output parameters such as von-Mises stress, equivalent plastic strain, extrusion contact pressure, heat flux and nodal temperature. The objective of the mesh convergence study is to ascertain the mesh size which will be utilized for FEM simulation of axisymmetric extrusion process, such that even after increasing the density of mesh (as number of elements along dimensions of workpiece increases, it will not affect the accuracy of FEM results). Mesh convergence study also aids in justifying accuracy of present FEM model as well. The criteria for selection of mesh size depends upon the convergence of all output parameters for such a common mesh size which would have good accuracy with less computational (CPU) time. Table 3 shows the mesh convergence results which provide data for all four parameters and list out total computational (CPU) time also. It is quite evident from Table 3 that mesh convergence is obtained for the partitioned mesh size 50×30 with good accuracy and lesser computational time. Besides, Table 3 also depicts that the two consecutive mesh sizes that 50×30 and 60×40 yielded similar numerical results which lies in a close proximity for all output field variable. In addition to it, Fig. 5 depicts two exact results for mesh size 50×30 and 60×40 especially for von Mises stress and conform the achievement of mesh convergence state. Since the mesh size 50×30 involves lesser number of elements and lesser computational time as compared to mesh size 60×40 with similar level of accuracy for numerical results, it can be easily chosen for FEM simulation of extrusion process. Thus this mesh size of 50×30 is suitable for FEM simulation of extrusion process which establishes present FEM model good enough for accurate prediction of numerical (FEM) results.

FEM simulation of extrusion process has been conducted using ABAQUS 6.14 software. Radius and length of initial billet prior extrusion are 100 mm and 300 mm respectively. Semi-angle of 56.5 ° with conical feature has been utilized herein. Die of extrusion process is modelled as rigid body (isothermal) while billet is modelled for obtaining deformation. Meshing of die and billet are done by employing CAX4T element types. Billet is moved in negative Y-direction through 250 mm by maintaining a constant velocity of 25 mm/s. Thermo-mechanical behavior of aluminium alloy for FEM simulation is governed by curves given as per Fig. 1. Friction coefficient during FEM simulation of extrusion process is taken as 0.1.Displacement boundary condition is applied on the reference point of the die, such that die remains static during whole FEM simulation. Again, displacement boundary condition is applied on the axisymmetric edge of billet, such that it also remains axisymmetric during the whole simulation. Third boundary displacement condition is applied on the upper most horizontal edge of the workpiece (i.e. on R_o) for downward movement of the billet by 0.125 mm for establishing contact at the interfaces at the start of simulation. Upper horizontal edge of billet is moved through 250 mm at rate of 25 mm/s. Thermal boundary condition is applied on the reference node of die to keep it on 20 °C, in order to behave as an isothermal rigid body. An initial condition in terms of predefined field of

[Downloaded from herasat.iust.ac.ir on 2025-07-19]

[DOI: 10.22068/ijmse.18.1.3]

temperature at 20 ˚C is assigned to the workpiece, such that the temperature of workpiece will be computed in later stages of FEM simulation. Entire simulation process is divided into multiple incremental steps. The Input parameters (with their range and values) considered in axisymmetric analysis of extrusion process are presented clearly in Table 4. Maximum nodal temperature and nodal temperature distribution, maximum heat flux and heat flux distribution are considered as presented as output parameters.

3. RESULTS AND DISCUSSION

3.1. Influence of Friction Coefficient

3.1.1. Influence of Friction Coefficient over Distribution of Temperature on Nodes

Fig. 6 shows influence of friction coefficient over distribution of temperature on nodes along the edge of billet which is in contact with die, i.e. from top to bottom. It is gathered from the Fig. 6 that the nodal temperature along edge of billet increases from top and attains a maximum value at location near half of the height of billet and from there, it decreases more or less linearly up to the bottom point of the billet. A similar pattern of variation in nodal temperature is gathered for all cases of friction coefficient. The minimum value of nodal temperature is obtained for lowest friction coefficient while highest temperature on nodes is observed for greatest friction coefficient. It is found that with increment in friction coefficient, the higher nodal temperature will be attained within billet at location near mid-point of the billet length. Higher will be friction coefficient between

Table 3. Mesh convergence data.

Mesh size	CPU Time (seconds)	Total no. of elements	Stress Mises	CPRESS	NT11	HFL	PEEQ
30×10	52.0	300	2.3060E+08	4.1630E+08	1.4500E+02	2.1840E+06	2.0050E+00
40×20	118.60	800	2.8320E+08	3.9560E+08	1.4860E+02	2.8660E+06	2.0380E+00
50×30	244.0	1530	2.2760E+08	3.9970E+08	1.4860E+02	2.9650E+06	2.0540E+00
60×40	423.00	2400	2.2760E+08	4.0240E+08	1.4960E+02	2.9930E+06	2.0780E+00
70×50	677.0	3500	2.3170E+08	4.0390E+08	1.5030E+02	3.0340E+06	2.0690E+00

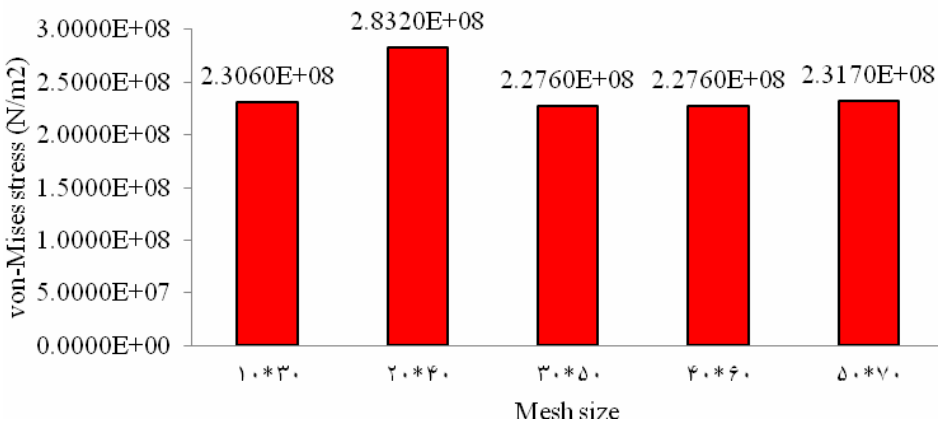

Fig. 5. von-Mises stress distribution for different mesh sizes

Table 4. Major inputs for FEM analysis [28].

Serial No.	Input parameters	Values	Range
1	Friction coefficient	μ = 0.0, 0.001, 0.025, 0.075, 0.1	μ= 0.0-0.1
2	Die angle (semi)	α = 45, 50, 55, 60 degrees	α = 45 to 60 degrees
3	Profile radii of die	R_p = 10, 12, 14, 16, 18, 20 mm	R_p = 10 to 20 mm
4	Predefined temperature (initial) of billet	T = 20, 25, 30, 35, 40, 45, 50 ˚C	T = 20 ˚C to 50 ˚C

[Downloaded from herasat.iust.ac.ir on 2025-07-19]

[DOI: 10.22068/ijmse.18.1.3]

interacting surfaces of die-billet assembly, greater will be the heat generation within billet which eventually results in increment in nodal temperature in billet.

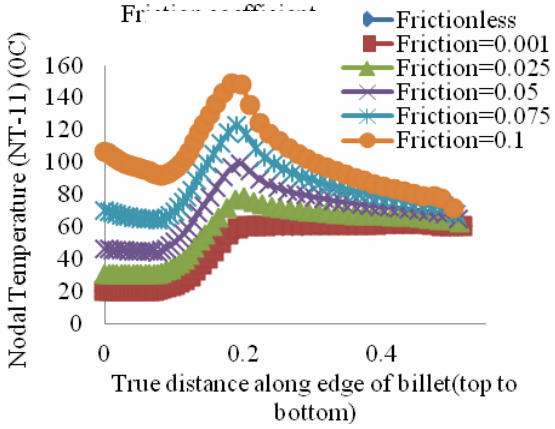

Fig. 6. Influence of friction coefficient on distribution of temperature on nodes (NT-11).

3.1.2. Influence of Friction Coefficient on Heat Flux Distribution

Fig. 7 shows influence of friction coefficient over heat flux distribution along a path from top to bottom of edge of billet, which is in contact with die surface. Generation of minimized heat flux is obtained for the cases of μ = 0.0 and 0.001, due to presence of lowest range of friction coefficient. Now upon increasing friction coefficient from μ= 0.001 and onwards, the heat flux distribution along edge of billet starts with a initial higher value and then again decreases gradually about a location near 20 % of length of billet from top portion of billet. It again starts increasing from there and attains a maximum value near a location of mid-point of billet. From this location near mid-point of billet length, heat flux again starts decreasing again up to the bottom end of the billet. It is found that higher will be the friction coefficient, higher will be the generation of heat flux within billet, as the maximum nodal temperature is achieved for highest friction coefficient.

3.1.3. Influence of Friction Coefficient on Maximum Nodal Temperature

Fig. 8 shows influence of friction coefficient over maximum temperature at nodes developed in the billet, as maximum nodal temperature increases quite predominantly by margin of nearly 129 % from state of frictionless to μ = 0.1.Higher friction coefficient results in attainment of peak temperature at nodes throughout billet, which signifies significant contribution of friction coefficient in elevation in temperature of billet.

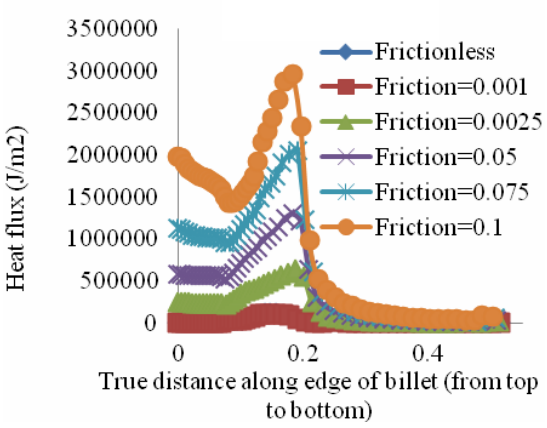

Fig. 7. Influence of friction coefficient on heat flux distribution.

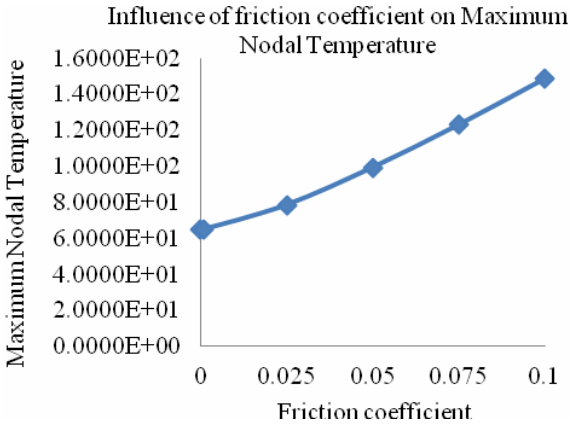

Fig. 8. Influence of friction coefficient on peak temperature at nodes.

3.1.4. Influence of Friction Coefficient on Peak Heat Flux

Fig. 9 shows the influence of friction coefficient over peak heat flux generated within the billet. It is worth to note that from the state of frictionless, nearly no maximum heat flux generated and it more or less varies linearly to attain a higher value with increment of friction coefficient .It is gathered from the Fig. 9, that friction coefficient contributes quite effectively in generation of maximum heat flux within billet as it also depends over peak temperature generated at nodes.

3.2. Influence of Die Angle

3.2.1. Influence of Die Angle on Peak Nodal Temperature

Fig. 10 depicts the influence of die angle on

[Downloaded from herasat.iust.ac.ir on 2025-07-19]

[DOI: 10.22068/ijmse.18.1.3]

maximum nodal temperature developed within billet. Maximum nodal temperature developed diminishes upon increment in die-angle (with horizontal) in range of α = 45˚, 50˚ and 55˚ and again increases with increase in die-angle from α = 55˚ to α = 60˚. It is found that maximum nodal temperature diminishes first with increment in semi-die- angle owing to easier navigation of material along profile radius of die, while upon further increment in semi-die angle causes greater frictional stresses within billet that results in rise in maximum temperature at nodes.

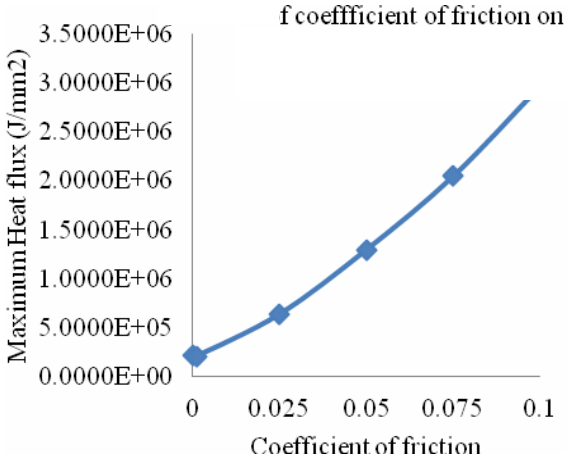

Fig. 9. Influence of friction coefficient on peak heat flux.

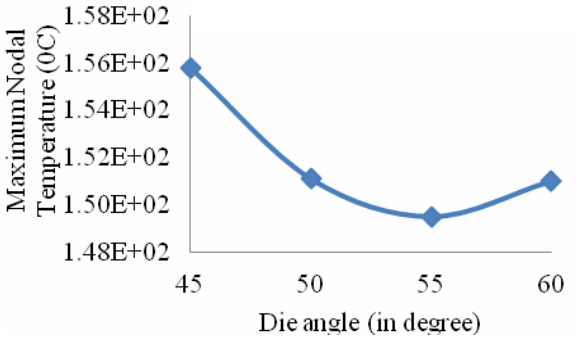

Fig. 10. Influence of die angle on peak nodal temperature.

3.2.2. Influence of Die Angle on Maximum Heat Flux

Fig. 11 depicts influence of die angle on maximum heat flux. Maximum heat flux developed diminishes upon increment in die-angle in range of α = 45˚, 50˚ and 55˚ and again increases with increase in die-angle from α = 55˚ to α = 60˚.It is found that maximum heat flux diminishes first upon rise in die- angle owing to easier of material flow along die profile radius as well as dependent on maximum nodal temperature, which actually decreases too. Later on increment in die-angle causes greater frictional stresses and maximum nodal temperature within billet, which contribute to increment in maximum nodal temperature within billet.

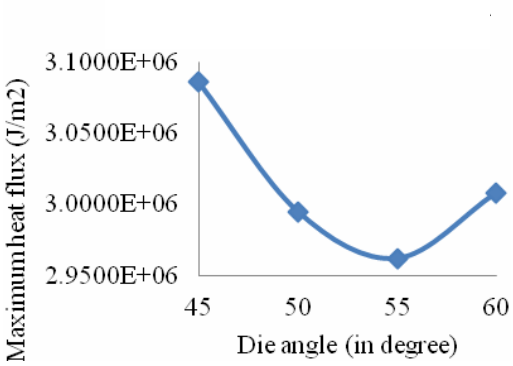

Fig. 11. Influence of die angle on maximum heat flux.

3.3. Influence of die profile radius

3.3.1. Influence of Die Profile Radius on Maximum Nodal Temperature

Fig. 12 shows the influence of die-profile radius on maximum nodal temperature developed. Maximum nodal temperature diminishes with increase in die profile radius by nearly 17 %. Higher will be the die profile radius easier will be the flow of material which in turn eventually cause decrement in maximum nodal temperature.

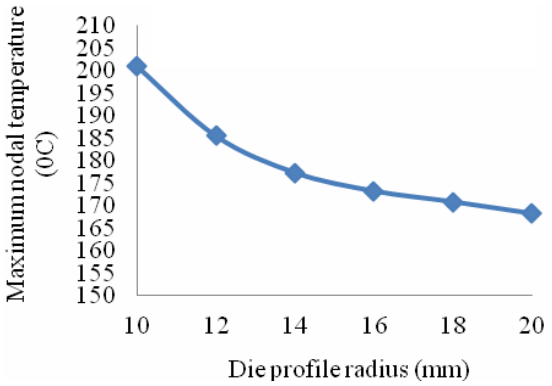

Fig. 12. Influence of die-profile radius on maximum nodal temperature.

3.3.2. Influence of Die Profile Radius on Maximum Heat Flux

Fig. 13 shows the influence of die-profile radius on maximum heat flux developed. Maximum heat flux diminishes non-linearly by 30% with increase in die profile radius. Higher will be the

[Downloaded from herasat.iust.ac.ir on 2025-07-19]

[DOI: 10.22068/ijmse.18.1.3]

die profile radius, lower will be the maximum heat flux developed in the billet.

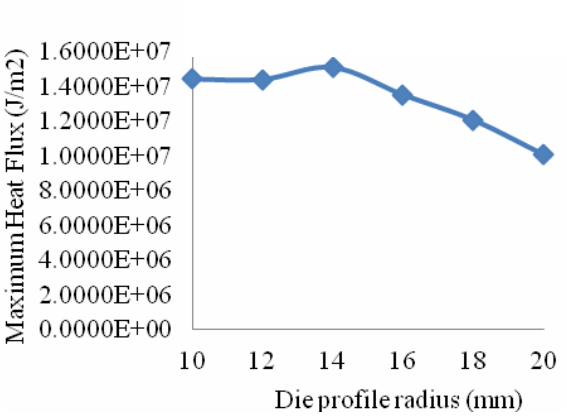

Fig. 13. Influence of die-profile radius on maximum heat flux.

3.4. Influence of predefined temperature of billet

3.4.1. Influence of Predefined Temperature of Workpiece on Maximum Temperature on Nodes

Fig. 14 shows influence of predefined temperature on maximum temperature on nodes developed. Maximum nodal temperature increases nearly linearly by 14 % with increment in predefined temperature of billet. Higher initial temperature of billet results in maximum temperature at nodes.

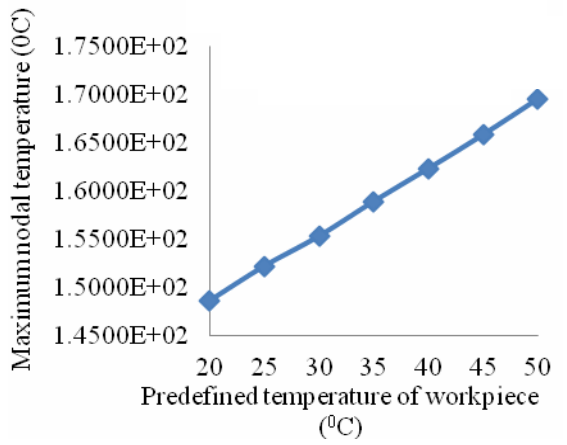

Fig. 14. Influence of predefined temperature of workpiece on maximum temperature on nodes.

3.4.2. Influence of Predefined Temperature of Workpiece on Maximum Heat Flux

Fig. 15 shows the influence of predefined temperature of billet on maximum heat flux developed in the billet. It is gathered from the Fig. 15 that maximum heat flux decreases non-linearly by 5 % with increment in the initial temperature of workpiece.

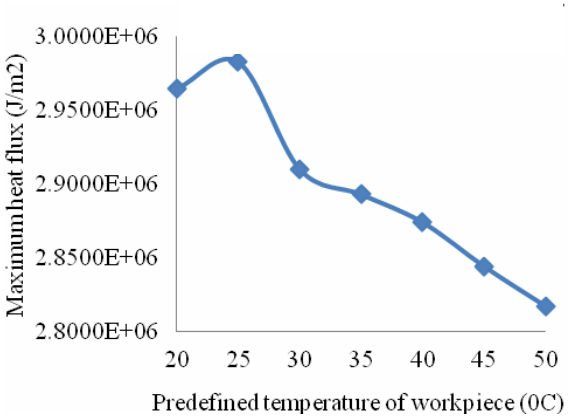

Fig. 15. Influence of predefined temperature of workpiece on maximum heat flux.

3.5. Comparison of Present Results with Previous Studies

Comparison of nodal temperature distribution w.r.t. friction coefficient is depicted in Fig. 16 with present FEM results with that of variation of friction coefficient with that results predicted by Kathirgamanathan and Neitzert" [27].The results of present FEM model presents that contour plots of nodal temperature distribution which clearly depicts that nodal temperature distribution increases with increment in friction coefficient. It is gathered that at lower friction coefficient i.e. from frictionless to friction coefficient = 0.1 (a-f), the zone of higher temperature goes on shrinking with a shift towards the die exit as per the results of present FEM model. In the similar manner, the nodal temperature distribution as per Kathirgamanathan and Neitzert [27] is given for friction coefficient = 0.05 and 0.25 in (g-h). Increment in nodal temperature distribution with a shift of peak values towards die exit is observed clearly irrespective of material properties and extrusion conditions. Higher will be the friction coefficient higher will be the resulting nodal temperature and there will be greater shift of maximum temperature towards die exit. Deformation behavior as well as trend of nodal temperature due to influence of friction coefficient of extrusion billet from present study match quite well with that of work of Kathirgamanathan and Neitzert [27].This proves the validity of present FEM model up to considerable extent.

[Downloaded from herasat.iust.ac.ir on 2025-07-19]

[DOI: 10.22068/ijmse.18.1.3]

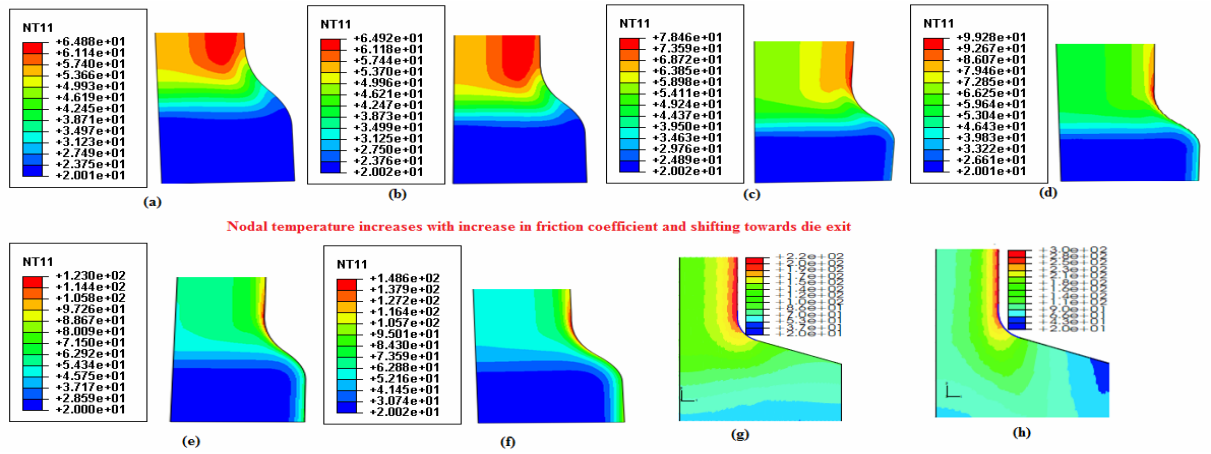

Fig. 16. Comparison of nodal temperature distribution of present FEM model (a-f) with Kathirgamanathan and Neitzert" [27] (g-f):
(a) μ = 0 (b) μ = 0.001 (c) μ = 0.025 (d) μ = 0.05 (e) μ = 0.075 (f) μ = 0.1 (g) μ = 0.05 (h) μ = 0.25

4. CONCLUSION

Finite element analysis of extrusion process has been carried out to study the thermo-mechanical behavior of aluminium alloy. The validation of present numerical model is established on the basis of deformation behavior in terms of evolution of nodal temperature distribution upon comparison with previous studies available in literature. Major findings of the research work can be summarized under the following sections:

1. Influence of friction coefficient
   - The higher the friction coefficient the higher is the increment in nodal temperature in billet.
   - It is found that the higher is the friction coefficient, the higher will be the generation of heat flux within billet, as this achieved for highest friction coefficient.
   - Maximum nodal temperature and maximum heat flux rises with increase in friction coefficient nearly by129 % and 131 % respectively.
2. Influence of Die-angle
   - It is found that maximum nodal temperature developed diminishes upon increase in die angle in range of α = 45˚, 50˚ and 55˚ and again increases with increase in die-angle from α = 55˚ to α = 60˚.
   - It is found that maximum heat flux diminishes first upon increase in die- angle owing to easier material flow along profile radius of die as well as dependent on maximum nodal temperature, which actually decreases too.
3. Influence of Die profile radius:
   - It is found that maximum nodal temperature diminishes with increase in die profile radius nearly by 17 %.
   - It is found that maximum heat flux diminishes non-linearly by 30% with increase in die profile radius.
4. Influence of Predefined temperature of billet:
   - It is gathered that maximum nodal temperature increases nearly linearly by 14 % with increment in predefined temperature of billet.
   - It is gathered that maximum heat flux decreases non-linearly by 5 % with increment in the initial temperature of workpiece.

REFERENCES

1. Lervik, A., Marioara, C. D., Kadanik, M., Walmsley, J. C., Milkereit, B. and Holmestad, R., (2020). "Precipitation in an extruded AA7003 aluminium alloy: Observations of 6xxx-type hardening phases". Mater. Des., 2020 ,186, 108204.
2. Singla, Y. K., Chhibber, R., Avdesh, Goyal, S. and Sharma, V. "Influence of single and dual particle reinforcements on the corrosion behavior of aluminum alloy based composites". P. I. Mech. Eng. L-J Mat., 2018 ,232 (6), 520-532.
3. Singh Yadav, R. K., Sharma, V. and Kumar, B. V. M. "On the role of sliding load and heat input conditions in friction stir processing on tribology of aluminium alloy–alumina surface composites". Tribol. Mater. Sur. & Inter., 2019, 13(2), 88-101.

[Downloaded from herasat.iust.ac.ir on 2025-07-19]

[DOI: 10.22068/ijmse.18.1.3]

4. Haase, M. and Tekkaya, A. E. “Recycling of aluminum chips by hot extrusion with subsequent cold extrusion”. Procedia Eng., 2014, 81, 652-657.
5. Liu, M., Zhang, C., He, H., Zhao, G., Chen, L. and Ma, X. “Interface microstructure evolution and mechanical properties of the extruded fiber-reinforced aluminum-based composite bar”. Mater. & Des., 2020,188, 108446.
6. Bai, S., Fang, G. and Zhou, J. “Construction of three-dimensional extrusion limit diagram for magnesium alloy using artificial neural network and its validation”. J. Mater. Process. Tech., 2020,275, 116361.
7. Greß, T., Mittler, T., Chen, H., Stahl, J., Schmid, S., Khalifa, N. B. and Volk, W. “Production of aluminum AA7075/6060 compounds by die casting and hot Extrusion”. J. Mater. Process. Tech., 2020, 280, 116594 .
8. Schikorra, M., Donati, L., Tomesani, L. and Kleiner, M. “ The role of friction in the extrusion of AA6060 aluminum alloy, process analysis and monitoring”. J. Mater. Process. Tech., 2007, 191(1-3), 288-292.
9. Eivani, A. R., Jafarian, H. R. and Zhou, J. “Simulation of peripheral coarse grain structure during hot extrusion of AA7020 aluminum alloy”. J. Manuf. Process., 2020, 57, 881-892.
10. Mackley, M.R. and Mulji ,N.C. “The axisymmetric extrusion of solid chocolate and the effect of die geometry”. Int. J. Form. Process., 2003, 6 (2),161-177.
11. Akhgar, J. M., Mirjalili, A. and Serajzadeh, S. "An Investigation into the Deformation Behaviour of AA6061-5% SiCp Composite During and after Hot Extrusion Process." P. I. Meh. Eng. L-J Mat., 2011, 225(1), 22-31.
12. Rattanochaikul, T., Janudom, S., Memongkol, N. and Wannasin, J. “Development of an aluminum semi-solid extrusion process”. J. Met. Mater. Miner., 2010, 20(2), 17-21.
13. Abrinia, K. and Orangi, S., Numerical study of backward extrusion process using finite element method.Finite Element Anaysis, ed. D. Moratal. Rijeka, Croatia, 2010, 381-406.
14. Parvizian, F., Schneidt, A., Svendsen, B. and Mahnken, R. “Thermo-mechanically coupled modeling and simulation of hot metal forming processes using adaptive remeshing method”. GAMM-Mitteilungen, 2010, 33(1), 95-115.
15. Chen, L., Zhao, G., Yu, J. and Zhang, W. “Constitutive analysis of homogenized 7005 aluminum alloy at evaluated temperature for extrusion process”. Mater. Des. , 2015, 66, 129-136.
16. Kapadia, N. and Desai, A. “Review on optimization study of die extrusion process using finite element method”. Int. J. Sci. Res. Develop., 2015, 3 (2): 2328-2330.
17. Dong, Y., Zhang, C., Zhao, G., Guan, Y., Gao, A. and Sun, W. “Constitutive equation and processing maps of an Al–Mg–Si aluminum alloy: Determination and application in simulating extrusion process of complex profiles”. Mater. Des, 2016, 92,983-97.
18. Ramezani, M. and Neitzert, T. “Computer simulations of direct extrusion of sintered Ti-6Al-4V alloy at elevated temperature”. Int. J. Appl. Eng. Res., 2016; 11(6), 3848-3852.
19. Hojda, S., Sturm, K.J., Terhorst, M., Klocke, F. and Hirt, G. “Damage dependent material properties in a finite element simulation of a hybrid forward extrusion process”. Procedia Eng., 2017, 207,437-441.
20. Wang, S.C., Zhang, X.H., Hu, X.L., Cai, Z.G. and Peng, B. “Study on the hot extrusion forming process of AZ31 magnesium alloy cylindrical shell”. Proceedings of the Int. Conf. on Advanced materials and energy sustainability (AMES’2016), 2017, 249-258.
21. Sahu, R.K., Das, R., Dash, B. and Routara. B.C. “Finite element analysis and experimental study on forward ,backward and forward-backward multi-hole extrusion process”. Mater. Today: Proc., 2018, 5(2), 5229-5234.
22. Zhou, W., Lin, J., Dean, T.A. and Wang, L. “Feasibility studies of a novel extrusion process for curved profiles: experimentation and modelling”. Int. J. Mach. Tools Manuf., 2018, 126, 27-43.
23. Zhang, H., Li, X., Deng, X., Reynolds, A.P. and Sutton, M.A. “Numerical simulation of friction extrusion process”. J. Mater. Process. Technol., 2018, 253, 17-26.

[Downloaded from herasat.iust.ac.ir on 2025-07-19]

[DOI: 10.22068/ijmse.18.1.3]

24. Yu, J., Zhang, Z., Wang, Q., Hao, H., Cui, J. and Li, L. "Rotary extrusion as a novel severe plastic deformation method for cylindrical tubes". Mater. Lett., 2018, 215, 195-199.
25. Chen, L., Liang, M., Zhao, G., Zhou, J. and Zhang, C. "Microstructure evolution of AZ91 alloy during hot extrusion process with various ram velocity". Vacuum, 2018, 150,136-143.
26. Kuboki, T., Ishikawa, M., Kajikawa, S. and Murata, M. "An extrusion method of tube with spiral inner fins by utilizing generation of spiral outer fins/grooves". CIRP Ann Manuf Technol, 2018, 67(1), 305-308.
27. Kathirgamanathan, P. and Neitzert, T. "Modelling of metal extrusion using ABAQUS" Proceedings of the 3rd New Zealand Metals Industry Conference, Hamilton, New Zealand, 2006, 1-9.
28. Yadav, R. R., Dewang, Y., Raghuwanshi, J. and Sharma, V. (2020). "Finite element analysis of extrusion process using aluminum alloy". Mater. Today: Proc., 2020, 24, 500-509.
29. Liu, M., Ji, Z., Fan, R. and Wang, X. "Finite element analysis of extrusion process for magnesium alloy internal threads with electromagnetic induction-Assisted heating and thread performance research". Mater. 2020, 13(9), 2170.
30. Preedawiphat, P., Mahayotsanun, N., Sucharitpwatskul, S., Funazuka, T., Takatsuji, N., Bureerat, S. and Dohda, K. "Finite Element Analysis of Grain Size Effects on Curvature in Micro-Extrusion". Appl. Sci., 2020. 10 (14), 4767.
31. Ataei, H., Shahbaz, M., Kim, H. S. and Pardis, N. "Finite Element Analysis of Severe Plastic Deformation by Rectangular Vortex Extrusion". Met. Mater. Int., 2020, in press, 1-7.
32. Park, N., Song, Y., Bae, G., Jung, S., Song, J., Lee, J. and Sung, H. "Evaluation of the effect of ram speed for extrusion of Al6063 based on ALE-based finite element analysis of L-shaped sample". Procedia Manuf.,2020, 50, 673-676.
33. Namburi, K. P. V., Kothasiri, A. F. and Yerubandi, V. S. M. "Modeling and simulation of Aluminum 1100 alloy in an extrusion process". Mater. Today: Proc., 2020, 23, 518-522.
34. Shukur, J. J. and Jaber, A. S. "Experimental and finite element analysis study of die geometrical affect the forming load during extrusion process". IOP Conf. Ser.: Mater. Sci. and Eng., 2020, 881(1), 012045.
35. Nouri, M., Semnani, H. M. and Emadoddin, E. "Computational and experimental studies on the effect back pressure on twist extrusion process". Met. Mater. Int., 2020, 1-9.
36. Davoudinejad, A., Bayat, M., Larsen, A., Pedersen, D. B., Hattel, J. H. and Tosello, G. "Mechanical properties of additively manufactured die with numerical analysis in extrusion process". AIP Conf. Proc., 2020, 2205 (1), 020006.

[Downloaded from herasat.iust.ac.ir on 2025-07-19]

[DOI: 10.22068/ijmse.18.1.3]